

Using Calcium Carbonate to Alter the Mechanical Properties of Recycled High Density Polyethylene

J. B. Koldsø, P. Kruse, R. H. Jermiin

Department of Materials and Production, Aalborg University
Fibigerstraede 16, DK-9220 Aalborg East, Denmark
jkolds15@student.aau.dk, Web page: <http://www.mechman.m-tech.aau.dk/>

Abstract

We have investigated how compatibilised calcium carbonate (CC) affects the mechanical and thermal properties of a recycled high density polyethylene (HDPE). The supplied CC was first characterised using infrared spectroscopy where a peroxide group was identified, possibly related to the compatibilising agent. Five blends of HDPE with 0 % to 40 % CC content, were compounded over two runs using a twin screw extruder.

Fractography inspections showed decent dispersion of particles and some agglomerates were identified for specimens with 10% and 20% filler. Fracture surfaces seemed brittle for all except 10% and 20% filler, that showed cavities of particles which was attributed to good matrix/filler bonding. Tensile tests showed the filler did not influence the material yield stress to a large degree, but could increase stiffness while decreasing ultimate elongation. Performing similar tests at elevated temperatures simply softened the material for all specimens, but CC was still able to affect the mechanical properties as for the tests at room temperature.

Keywords: Recycled High Density Polyethylene (rHDPE); Calcium Carbonate; Characterisation; Infrared Spectroscopy; Fractography; Mechanical Properties

1. Introduction

Plastic is incorporated to an increasing degree in consumer products because of its excellent properties and high durability [1]. Following use of the product discarded plastic is often not dealt with appropriately, which poses an environmental problem [1, 2, 3]. Polyethylene is the most common plastic in the world [1] and thus could be expected to be abundant as discarded material. A solution to the problem would be to increase the intended lifetime of the materials by collecting and reusing the discarded plastic.

Plastic, which have been exposed to nature and the elements for a longer period of time, will typically have inferior properties compared to the virgin material, as a result of degradation, this becomes a problem when implementing it in new products [4]. The degree and cause of degradation will vary depending on the environment the plastic has been subjected to, complicating its use in products that require consistent material quality. Plastic can degrade due to different external exposures, so additives are often added to counteract fx. degradation as a result of UV-radiation or thermal exposure [1].

Recycled plastic can also be modified to improve

its mechanical properties and make it more suitable for incorporation in new products and the challenge becomes choosing a proper modification. Incorporating strengthening additives, such as fibres or mineral fillers, is an accessible method, provided the blend can be compatibilised properly - ensuring interaction between filler and matrix [5]. CC is a well-known and commonly added filler used for increasing stiffness and impact strength, reducing shrinkage, and counteracting dimensional instability (warpage) [6, 7]. This article will be dealing with the addition of a CC filler to a recycled HDPE matrix.

Adding fillers to a polymer generally affects both its mechanical and thermal properties. CC filler tend to increase stiffness, density and viscosity of the material system while simultaneously increasing heat of fusion [6, 8]. An HDPE with ethylene oxide oligomer modified CC was shown to increase both stiffness and yield strength in [9]. [8] achieved a minor increase in yield strength by treating CC with stearic acid. Increased stiffness but reduced yield strength was observed by [10, 11] for CC treated with calcium stearate. In all cases, a compatibilisation treatment had been carried out in order to improve matrix-filler interface. Variation in the compatibilisation method can create composites

with different mechanical properties because of varying interface qualities. Agglomeration of particles and poor matrix-filler adhesion reduce mechanical strength of composites [8, 12]. Untreated polyethylene and CC have different polarities and thus will only interact mechanically through friction and entanglement [5, 13]. The matrix-filler affinity can be modified by changing their polarity, which ensures at least a secondary bond between the two. Alternatively, a third component which have an affinity with both filler and matrix can be added [10, 11].

Looking into morphological properties of the composite shows that an increase in mechanical strength is to be expected as the degree of crystallisation is raised [1, 14, 15]. An increase in crystallinity with increasing CC content was seen in [8, 10] and was attributed to the nucleation-promoting properties of the particles [6]. When macromolecules are becoming ordered and forming crystals the overall material density is increasing leading to volumetric shrinkage of the entire specimen [1]. Adding nano-sized CC particulates could reduce shrinkage in polypropylene and was attributed to the presence of more heterogeneous nucleation sites. Exceeding a threshold concentration of particles lead to particle agglomeration and consequently less nucleation sites and hence fewer crystals and more shrinkage [16, 17].

The present article deals with recycled HDPE made from fishing nets and trawl acquired from oceans, that have been sorted, cleaned, and re-extruded into new pellets. CC, sourced as a waste product from a marble quarry, will be added. The purpose will be to study how the filler can be used to modify the properties of the recycled plastic. The material properties will be examined at varying concentrations of added CC in order to find a possible optimum. Further investigations will be made to explain how the mechanical properties change according to material microstructure morphology.

2. Experimental

2.1 Materials

The calcium carbonate was supplied as pellets with polyethylene/polypropylene from Omya under the brand name Omyalene 102M-OM. An unknown polyolefin/calcium carbonate compatibiliser has already been added by the supplier. The calcium carbonate was a crystalline calcite sourced from a quarry (GCC) with a median particle diameter of 2 μm and maximum of 10 μm . The recycled HDPE was supplied by Plastix and

branded OceanIX rHDPE0507. It was too viscous to injection mould and Plastix opted to add a less viscous, virgin polyethylene at a one to one ratio. This was supplied by Sabic and branded as HDPE CC3054.

2.2 Processing

Five 500 g batches of granulate were prepared with a calcium carbonate content of 0% to 40% at 10% intervals. OceanIX and Omyalene was weighed off and manually shaken together in a bucket until evenly dispersed. Each mixture was manually fed in a Thermo Scientific Prism Eurolab 16 twin screw extruder with settings as shown in Table I. Parameters were first determined from [18], but adjusted to the specific mixture. The extruded melt was manually lead through a cooling waterbath, rolled to a coil and left to dry at room temperature until next morning where the thread was granulated. This extrusion process was repeated once.

Parameter	Value	Unit
Barrel temperature - all zones	200	$^{\circ}\text{C}$
Die pressure	~50	bar
Screw speed	~50	rpm
Screw power	~1.4	kW

Tab. I Extrusion parameters

The prepared granulate was injection moulded using a piston-driven Thermo Scientific Haake Minijet II with process parameters as shown in Table II. Parameters were found by moulding dummy specimens until a reproducible specimen appearance was found. Specimens were moulded in the shape of design 5A as mentioned in [19] and immediately placed on a table under a cold steel plate for 5 min to avoid warpage. Specimens were then kept at room temperature for 48 h before testing.

Parameter	Value	Unit
Cylinder temperature	180	$^{\circ}\text{C}$
Mould temperature	60	$^{\circ}\text{C}$
Melt time	3	min
Injection pressure	500	bar
Holding pressure	500	bar
Holding time	10	s

Tab. II Mould parameters

2.3 Testing

Infrared (IR) spectra were obtained with a Bruker LUMOS IR microscope.

Fractography inspections were carried out on 10 mm \times 3 mm \times 78 mm specimens left in liquid nitrogen (-200°C) for 15 min. After cooling, specimens were hit with a hammer and chisel and

the fracture surfaces were coated with gold using a Edwards S150B sputter coater and then inspected using a Zeiss EVO 60 scanning electron microscope (SEM).

Rheology tests were carried out on a Discovery HR3 from TA Instruments. They were performed with frequency sweeps from 600 rads^{-1} to 0.06 rads^{-1} and maximum strain was 5% at a temperature of 180°C .

Non-heated tensile tests were performed on a Zwick Z100 with a 100 kN loading cell. The test were made according to [19] and relevant numbers were determined as mentioned in the standard. Heated tensile tests were performed on an Instron 5568 with attached air-heated oven from Instron and the specimens and method were the same as used for the non-heated tests.

DSC tests were performed on a Q2000 from TA Instruments using 4 mg to 6.3 mg cubes cut from injection moulded sticks so they only consisted of core material. Temperature was varied in three intervals; heat from 20°C to 250°C , cool 250°C to -70°C and heat -70°C to 250°C , all at $10^\circ\text{C min}^{-1}$.

TGA tests were performed on a SDT 650 from TA Instruments using plastic granulates weighing 16 mg to 25 mg heated to 1000°C at 5°C min^{-1} .

2.4 Characterisation

The supplied CC was inspected using IR spectroscopy and the resulting spectrum, along with that of pure CC, can be seen on Figure 1. A pure CC sample was acquired by heating an Omyalene pellet to 500°C so as to burn away all other compounds while avoiding calcination of the CC. Peaks were identified using OriginLab software and peak wave numbers are mentioned in Table III.

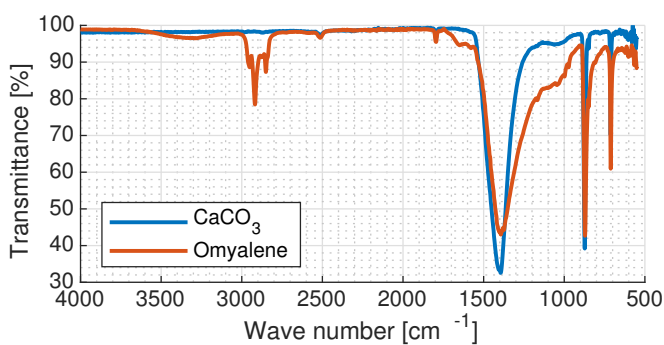


Fig. 1 IR spectrum of Omyalene 102M

Pure calcite have been inspected in [20], where peaks related to vibration modes of the crystals were found. Corresponding peaks were found in the sample at hand

and can be attributed to the presence of calcite. Some peaks related to the polyethylene has been assigned according to [21, 22], but only stretch modes were identifiable. Other mode peaks lie close to peaks related to calcite and are obscured by them. Shoulders were observed on the Omyalene spectrum around 1100 cm^{-1} and 850 cm^{-1} which have been identified according to [22] as bonds of peroxides groups.

Peroxide groups act as free radical initiators during the polymerisation process [23], but may also be related to the matrix/filler compatibilisation treatment as mentioned in [5, 24].

Wave number	Reference	Assignment
711	713	Calcite
869	877	
1391	1420	
850	900 - 800	O–O stretch
1104	1150 - 1030	C–O stretch
2847	2880 - 2840	R–CH ₂ –R stretch
2919	2950 - 2920	
2890	2880 - 2850	R–CH ₃ stretch
2955	2960 - 2930	

Tab. III Peaks identified in the Omyalene IR spectrum.

3. Results and discussion

3.1 Fractography

All images shown have been aligned so the impact direction is vertical going upwards. Images were taken at the very end of the fracture surface, furthest from the crack initiation site.

A sample without added filler was inspected and can be seen on Figure 2. Scattered across the fracture surface are inclusions of contaminants such as sand particles, inferred since the plastic has been subjected to oceanic environments. The flaky appearance of the area indicates a brittle-like fracture [25] and there is no overall direction of crack growth.

Adding 10% calcium carbonate gives a fracture surface shown on Figure 3. Flakes have become less distinct and cavities of plastic with particles lodged in the middle, have appeared. The particle type is indistinguishable, but the cavities appear only when calcium carbonate is added, suggesting a relation. Cavities are associated with matrix/filler debonding indicating an interface had been made [10]. Fibrillation, as seen from how the matrix has been pulled around the particle is a sign of plastic deformation [25] and indicates a ductile fracture

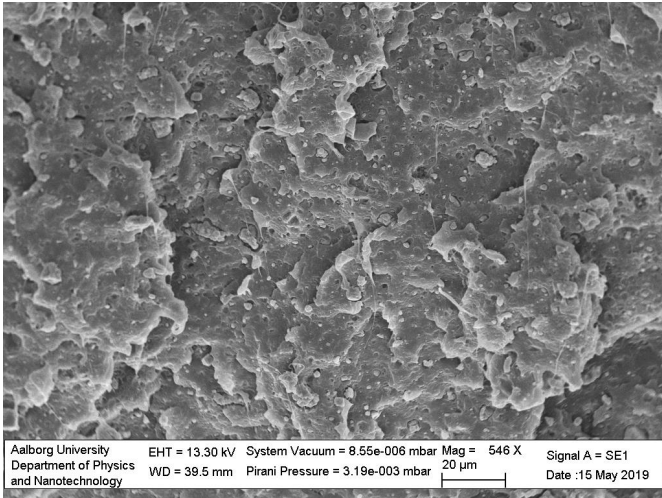


Fig. 2 SEM image of the fracture surface of a specimen with no filler.

mode. Long fibrils can be seen in the top of the image emphasising the ductile behaviour of the material.

A rather large particle deposit can be seen as highlighted in red on Figure 3. Its size, larger than the maximum CC particle size of 10 µm, indicates it is not a single particle, but rather an agglomeration of calcium carbonate particles. It cannot be a sand particle, since it is situated in a cavity and must then previously have bonded with the matrix.

Increasing the filler content to 20% yields the fracture seen on Figure 4. A denser concentration of cavities is seen, which could be attributed to an increase in CC concentration. Agglomerates can still be seen. Several strings of plastic can also be seen going vertically from the top of the image highlighting the direction of impact.

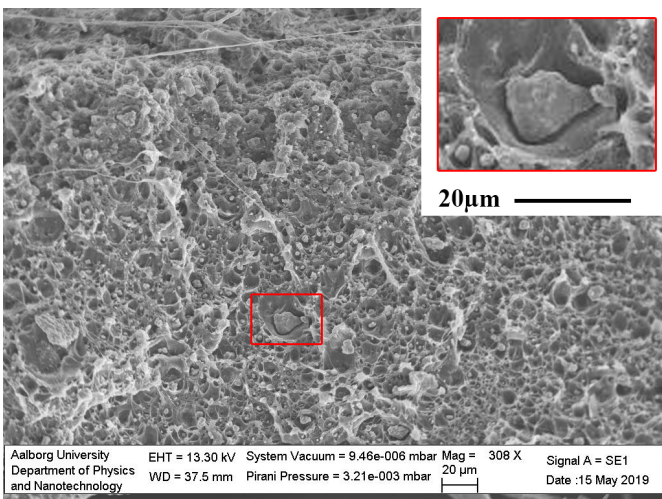


Fig. 3 SEM image of the fracture surface of a specimen with 10% filler.

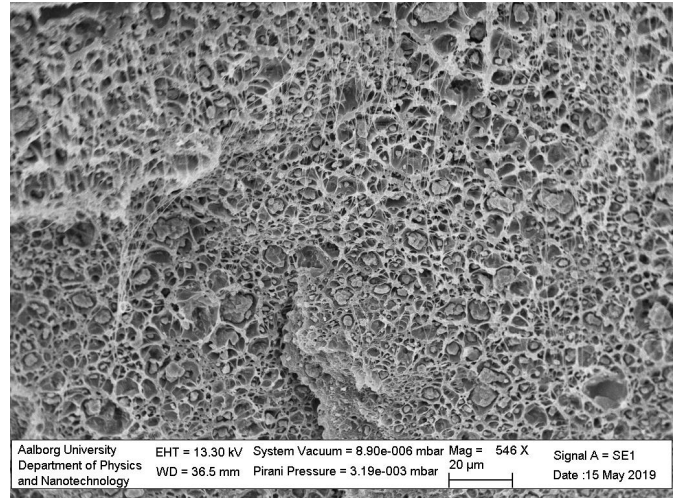


Fig. 4 SEM image of the fracture surface of a specimen with 20 filler.

A distinct change in landscape is seen for the 30% filler specimen seen on Figure 5. Flakes have reappeared and the cavities phenomenon is no longer apparent. The material has become more brittle as a consequence of the high filler content and the plastic is no longer allowed to deform significantly before fracture. A similar landscape is seen for 40% CC content on Figure 6.

In general, specimens with 10% and 20% filler appear tougher because more micro plasticity is apparent.

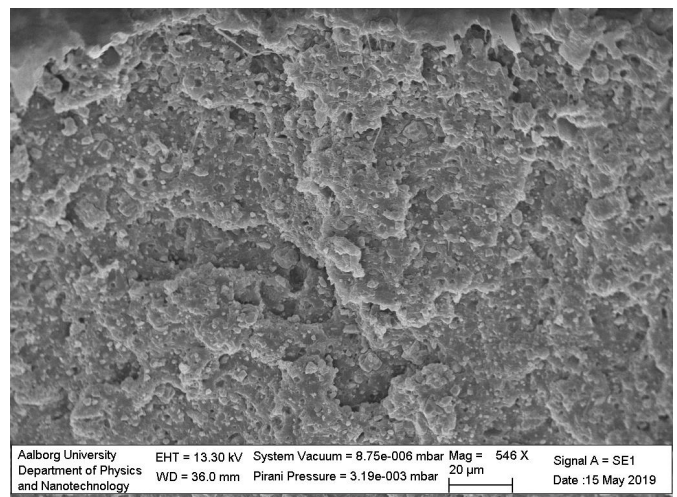


Fig. 5 SEM image of the fracture surface of a specimen with 30 filler.

3.2 Rheology

The rheology measurements seen on Figure 7, where specimens with 0% and 10% filler have identical curves. Going from right to left, all curves are seen approaching a plateau, but the 0% and 10% are have

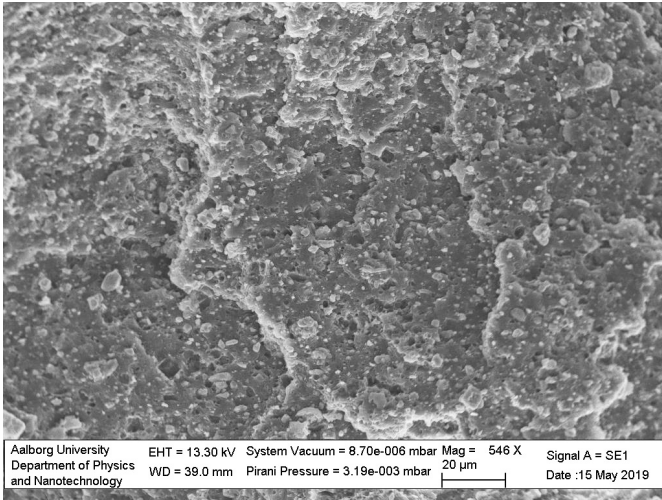


Fig. 6 SEM image of the fracture surface of a specimen with 40 filler.

the lowest slope at those points. No sudden increase in complex viscosity was observed at low angular velocity, indicating the fluid is not acting as a Bingham fluid. Seeing phenomenon akin to Bingham fluids indicate the presence of a strong matrix/filler bond as mentioned in [26, 27, 28]. Fractography measurements confirmed the presence of bonds, however the rheology data indicates weak bonding.

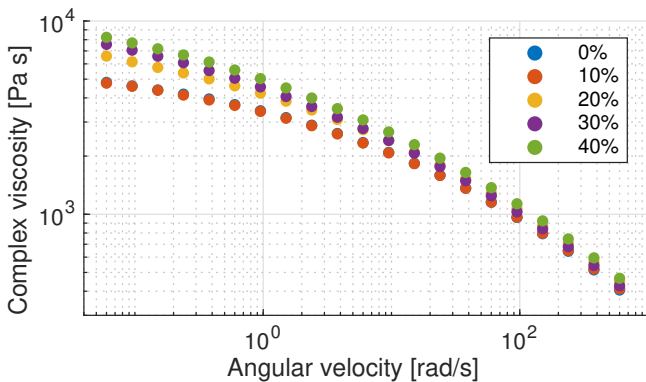


Fig. 7 The resulting results curves from the rheology experiment.

3.3 Tensile

Results from the tensile tests performed at 20 °C, 80 °C, and 100 °C can be seen on Figure 8, 9, and 10, respectively. Strains are determined from the initial gauge length of 20 mm. Some specimens did not fracture at maximum extension; these are marked with a triangle. The curves shown were chosen so as to be representative of the observed tendencies, but high variations were seen for specimens at elevated temperatures, so the most frequently observed curve type was chosen. Key figures were calculated according

to [19] and are shown in Table IV. A two way analysis of variance was carried out for the relations between each calculated mechanical property, temperature, filler content, and interactions. The highest p-value found was 0.0013, so both temperature and filler content has a statistically significant impact on stiffness, yield strength and ultimate elongation.

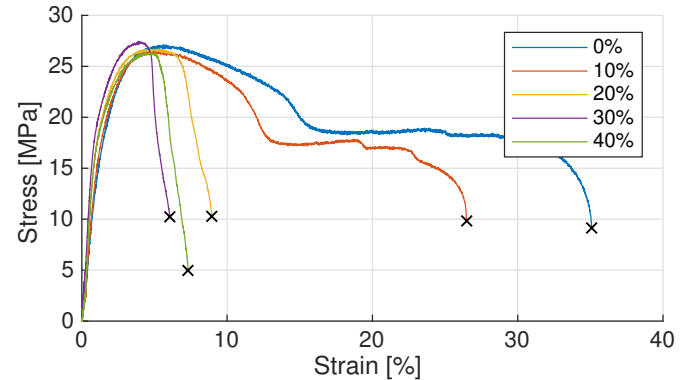


Fig. 8 Representative stress-strain curves for testing at room temperature.

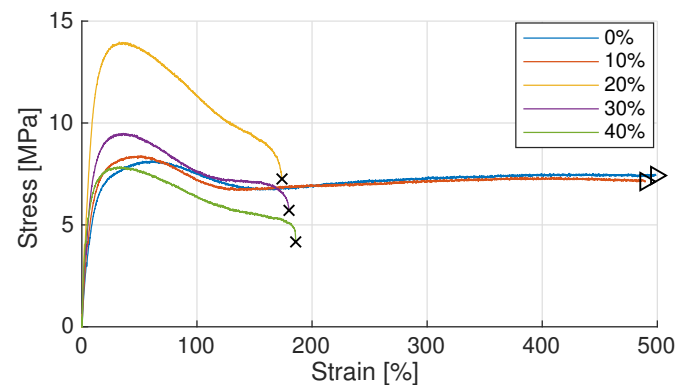


Fig. 9 Representative stress-strain curves for testing at 80 °C.

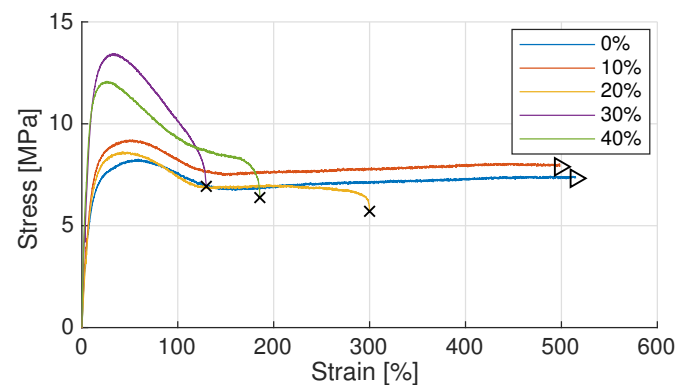


Fig. 10 Representative stress-strain curves for testing at 100 °C.

Looking at the data from the room temperature tests, a threshold particle content is seen in terms of ultimate

CaCO ₃ [%]	T [°C]	Yield stress [MPa]		E-modulus [MPa]		Ultimate elongation [%]	
		Mean	σ	Mean	σ	Mean	σ
0%	20	27.4	0.2	954.5	93.5	32.4	2.9
	80	8.8	2.8	169.7	53.7	518.1	37.5
	100	8.4	0.5	82.0	12.2	513.6	16.4
10%	20	26.2	0.3	840.7	48.1	31.3	7.2
	80	10.7	1.0	171.8	32.0	510.8	8.5
	100	8.9	0.5	78.6	10.6	496.0	4.8
20%	20	26.8	0.5	1306.6	40.5	10.7	1.2
	80	16.2	4.0	222.4	50.8	268.6	151.9
	100	10.0	2.2	135.8	38.6	315.6	110.3
30%	20	26.8	2.2	1497.3	165.6	7.5	0.4
	80	13.8	3.5	448.8	144.6	52.6	33.2
	100	10.4	1.7	157.7	36.0	169.0	23.7
40%	20	25.8	0.8	1412.9	188.9	8.3	1.0
	80	15.1	1.3	201.7	60.7	127.1	28.7
	100	12.6	4.4	214.7	62.5	159.9	29.5

Tab. IV Relevant mechanical properties determined from tensile tests.

elongation and stiffness. Specimens with more than 10% CC content had increased stiffness and reduced ultimate elongation, but no significant increase in yield stress. This effect is apparent across all environment temperatures and could be attributed to an increased degree of crystallisation. Increasing the temperature to 80 °C does not change the threshold behaviour, but simply softens all specimens. At this temperature, specimens below 20% CC content have fairly similar looking curves while above 20%, high degrees of variation are seen. Further increasing the temperature to 100 °C does not pronounce the effects seen significantly, but high variation is still seen. The variation may be attributed to the influence micro defects have on mechanical behaviour in the beginning of the load cycle. Micro defects, such as contaminants, initiate a yield zone that will increase in size at elevated temperatures and thus makes the material more sensitive to the particular defect.

3.4 TGA/DSC

Results from the TGA tests performed in an atmosphere of air and nitrogen can be seen on Figure 11 and 12, respectively. The calculated onset temperature for decomposition, can be seen on Figure 13 along with melt onsets calculated from DSC data. All temperatures are calculated from the inflection point between transition peak slope and extrapolated baseline. Temperatures are presented normalised according to their mean transition temperature. Decomposition temperature of samples without filler was 395 °C and 469 °C for air and nitrogen atmosphere, respectively, while melt onset was 120 °C. The melt onset was only found in an nitrogen atmosphere using DSC.

The tests show some increase in decomposition temper-

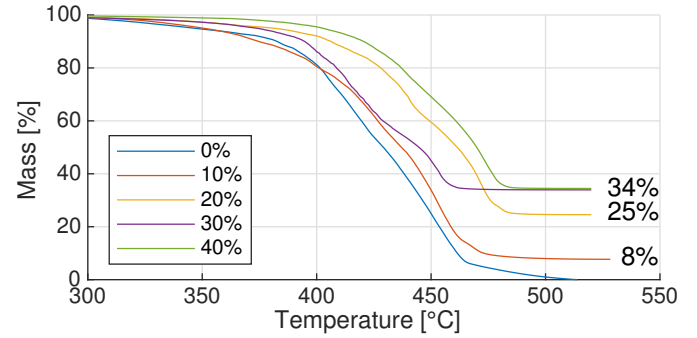


Fig. 11 Results of TGA on specimens in air, containing differing amounts of calcium carbonate.

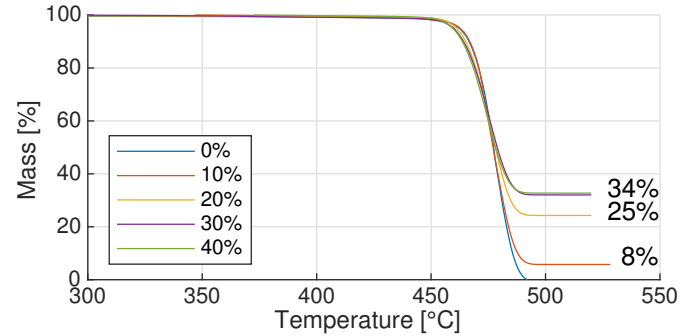


Fig. 12 Results of TGA on specimens in nitrogen, containing differing amounts of calcium carbonate.

ature in air with increased filler content, except for an inconsistency with 30%. Compatibiliser concentration could be affecting these changes, as seen in [29] were compatibiliser interface bond energy and decomposition temperature were related. Decomposition temperature seem invariant to filler content when in a nitrogen atmosphere.

An assessment of the actual CC concentration in the sample was made from the final weight percentage above 500 °C as this represents the leftover CC. It is

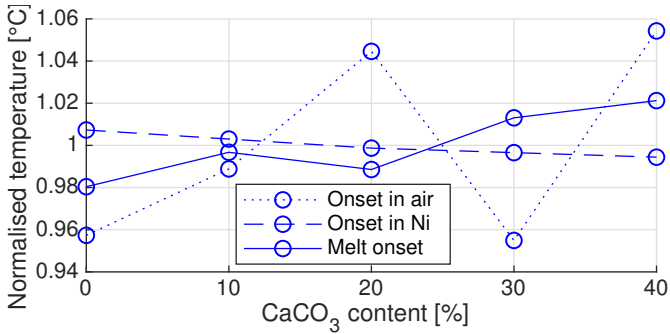


Fig. 13 Normalised decomposition onset temperatures determined from TGA along with melt onset temperatures determined from DSC.

seen, that the actual filler weight percentage was not as expected for several of the specimens. This is attributed to poor mixing of particles in the plastic blend due to insufficient compounding.

All measured DSC curves had similar appearance, so a characteristic DSC curve is shown on Figure 14, where significant sites have been appointed. Melting is seen at *a*, peroxide reaction at *b* and recrystallisation at *c* [1]. The peroxide reaction peak was only observed for 0% and 20% filler content which can be attributed to the presence of contaminants. Peroxides were known to be present in the Omyalene, but since none is added for 0%, the reaction must be caused by something else.

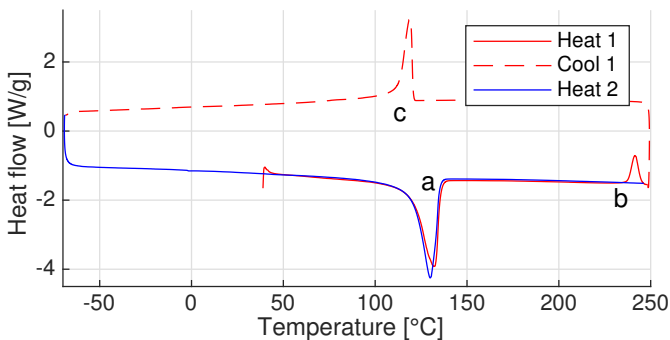


Fig. 14 Characteristic DSC curve (Exothermic up).

Peaks of melting and recrystallisation have been integrated across the extrapolated baseline to find the enthalpy of fusion, ΔH , which is used to find degree of crystallisation, x_C by

$$x_C = \frac{\Delta H}{\Delta H_\infty x_p} \quad (1)$$

where ΔH_∞ is the enthalpy of fusion at maximum degree of crystallisation, found from [30] to be 307 J g^{-1} . x_p is the plastic weight fraction incorporated to account for the filler content, that is not able to crystallise and thus lower the maximum enthalpy of fusion. The actual

filler content found from the TGA data has been used for x_p . Calculated values of crystallinity can be seen on Figure 15 and it is seen that there might be a relation between filler content and crystallinity. The tensile test showed a higher yield strength at 10% and 20%, but this is not consistent with the DSC data, as only 10% shows a larger amount of crystals present.

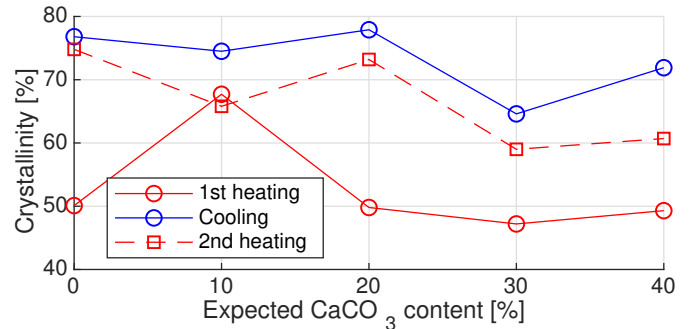


Fig. 15 Degree of crystallisation for varying CC concentration.

CC particles promote heterogeneous nucleation [8, 10], but the growth could be stunted by particle agglomeration that lead to a net decrease in nucleation sites. This could explain why only 10% filler show an increased degree of crystallinity, as the amount of agglomerates is sufficiently low. During cooling and second heating interval, there seem to be no distinctive pattern in the degree of crystallisation, but it is generally higher compared to that of the first heating interval. Low cooling rates allow for crystals to form and could be low enough for homogeneous nucleation to occur and crystallinity becomes invariant to particle content.

4. Conclusion

The supplied Omyalene was found to contain a binding agent with a peroxide group. However, rheology measurements showed that the HDPE/CC bonding was weak. It was found, the filler acted as thermal stabiliser, increasing decomposition and melt onset in air. Additionally, particles were found to increase degree of crystallisation at a concentration of 10% owing to its nucleation effects. Increased stiffness and decreased ultimate elongation was seen with increased CC content for 20 °C, 80 °C, and 100 °C.

Acknowledgement

The authors of this work gratefully acknowledge Grundfos for sponsoring the 7th MechMan symposium.

References

- [1] T. A. Osswald and G. Menges, *Materials Science of Polymers for Engineers*. Carl Hanser, 3rd ed., 2012.
- [2] J. Hopewell, R. Dvorak, and E. Kosior, "Plastics recycling: challenges and opportunities," *Philosophical Transactions of the Royal Society B: Biological Sciences*, vol. 364, no. 1526, pp. 2115–2126, 2009.
- [3] R. M. Bajracharya, A. C. Manalo, W. Karunasena, and K.-t. Lau, "Characterisation of recycled mixed plastic solid wastes: Coupon and full-scale investigation," *Waste management*, vol. 48, pp. 72–80, 2016.
- [4] M. L. Maspoch, H. E. Ferrando, and J. I. Velasco, "Characterisation of filled and recycled pa6," in *Macromolecular Symposia*, vol. 194, pp. 295–304, Wiley Online Library, 2003.
- [5] M. Xanthos, "Interfacial agents for multiphase polymer systems: recent advances," *Polymer Engineering & Science*, vol. 28, no. 21, pp. 1392–1400, 1988.
- [6] R. Rothon, *Fillers for polymer applications*. Springer, 2017.
- [7] O. AG, "Omyaweb molding," 2014.
- [8] Z. Cao, M. Daly, L. Clémence, L. M. Geever, I. Major, C. L. Higginbotham, and D. M. Devine, "Chemical surface modification of calcium carbonate particles with stearic acid using different treating methods," *Applied Surface Science*, vol. 378, pp. 320–329, 2016.
- [9] B. M. Badran, A. Galeski, and M. Kryszewski, "High-density polyethylene filled with modified chalk," *Journal of Applied Polymer Science*, vol. 27, 1982.
- [10] Z. Bartzak, A. Argon, R. Cohen, and M. Weinberg, "Toughness mechanism in semi-crystalline polymer blends: Ii. high-density polyethylene toughened with calcium carbonate filler particles," *Polymer*, vol. 40, no. 9, pp. 2347–2365, 1999.
- [11] E. Parsons, M. Boyce, D. Parks, and M. Weinberg, "Three-dimensional large-strain tensile deformation of neat and calcium carbonate-filled high-density polyethylene," *Polymer*, vol. 46, no. 7, pp. 2257–2265, 2005.
- [12] S. Sahebian, S. M. Zebarjad, S. A. Sajjadi, Z. Sherfat, and A. Lazzeri, "Effect of both uncoated and coated calcium carbonate on fracture toughness of hdpe/caco3 nanocomposites," *Journal of Applied Polymer Science*, vol. 104, no. 6, pp. 3688–3694, 2007.
- [13] L. Domka, A. Wąsicki, and M. Kozak, "The microstructure and mechanical properties of new hdpe-chalk composites," *Physicochemical problems of mineral processing*, vol. 37, pp. 141–147, 2003.
- [14] M. P. Stevens, *Polymer chemistry an introduction*. Oxford, 2009.
- [15] J. Charles E. Carraher, *Carraher's Polymer Chemistry*. CRC Press, tenth ed., 2018.
- [16] K. Shelesh-Nezhad, H. Orang, and M. Motallebi, "Crystallization, shrinkage and mechanical characteristics of polypropylene/caco3 nanocomposites," *Journal of Thermoplastic Composite Materials*, vol. 26, no. 4, pp. 544–554, 2013.
- [17] Y.-J. Xu, W. Yang, B.-H. Xie, Z.-Y. Liu, and M.-B. Yang, "Effect of injection parameters and addition of nanoscale materials on the shrinkage of polypropylene copolymer," *Journal of Macromolecular Science@*, vol. 48, no. 3, pp. 573–586, 2009.
- [18] J. Musil and M. Zatloukal, "Experimental investigation of flow induced molecular weight fractionation during extrusion of hdpe polymer melts," *Chemical engineering science*, vol. 66, no. 20, pp. 4814–4823, 2011.
- [19] ISO-527, "Plastics - determination of tensile properties," standard, International Organization for Standardization, Geneva, CH, 2012.
- [20] F. A. Andersen, L. Brecevic, et al., "Infrared spectra of amorphous and crystalline calcium carbonate," *Acta Chem. Scand*, vol. 45, no. 10, pp. 1018–1024, 1991.
- [21] P. Larkin, *Infrared and Raman Spectroscopy*. Elsevier, 2017.
- [22] G. Socrates, *Infrared and Raman Characteristic Group Frequencies*. John Wiley and Sons Ltd, 2004.
- [23] M. P. Stevens, *Polymer chemistry an introduction*. Oxford University Press, 2009.
- [24] A. O. Baranov, A. V. Kotova, A. N. Zelenetskii, and E. V. Prut, "The influence of the nature of the chemical reaction on the structure and properties of blends in the reactive blending of polymers," *Russian chemical reviews*, vol. 66, no. 10, p. 877, 1997.
- [25] C. Deshmane, Q. Yuan, and R. Misra, "On the fracture characteristics of impact tested high density polyethylene–calcium carbonate nanocomposites," *Materials Science and Engineering: A*, vol. 452, pp. 592–601, 2007.
- [26] H. Barnes, *A Handbook of Elementary Rheology*. Raymond F. Boyer Library Collection, University of Wales, Institute of Non-Newtonian Fluid Mechanics, 2000.
- [27] A. Shenoy, *Rheology of Filled Polymer Systems*. Springer, 1999.
- [28] R. Klitkou, E. A. Jensen, and J. d. C. Christiansen, "Effect of multiple extrusions on the impact properties of polypropylene/clay nanocomposites," *Journal of Applied Polymer Science*, vol. 126, no. 2, pp. 620–630, 2012.
- [29] R. Jana, P. Mukunda, and G. Nando, "Thermogravimetric analysis of compatibilized blends of low density polyethylene and poly (dimethyl siloxane) rubber," *Polymer degradation and stability*, vol. 80, no. 1, pp. 75–82, 2003.
- [30] C. Atkinson and M. Richardson, "Thermodynamic properties of ideally crystalline polyethylene," *Transactions of the Faraday Society*, vol. 65, pp. 1764–1773, 1969.